MOLECULAR AND CELLULAR BIOLOGY, Feb. 2006, p. 1527–1537 Vol. 26, No. 4
0270-7306/06/$08.00+0 doi:10.1128/MCB.26.4.1527–1537.2006

An E2F Binding-Deficient Rb1 Protein Partially Rescues Developmental Defects Associated with Rb1 Nullizygosity†

Huifang Sun,[1]‡ Yanjie Chang,[1]‡ Brett Schweers,[2] Michael A. Dyer,[2] Xiaojing Zhang,[1] Simon W. Hayward,[3] and David W. Goodrich[1]*

Department of Pharmacology & Therapeutics, Roswell Park Cancer Institute, Buffalo, New York 14263[1]; Department of Developmental Neurobiology, St. Jude Children's Research Hospital, Memphis, Tennessee 38105[2]; and Departments of Urologic Surgery and Cancer Biology, Vanderbilt University Medical Center, Nashville, Tennessee 37235[3]

Received 31 August 2005/Returned for modification 8 October 2005/Accepted 4 December 2005

***Rb1* is essential for normal embryonic development, as null mice die in midgestation with widespread unscheduled cell proliferation. *Rb1* protein (pRb) mediates cell cycle control by binding E2F transcription factors and repressing expression from E2F-dependent promoters. An increasing amount of evidence suggests that pRb loss also compromises cellular differentiation. Since differentiation is often dependent on cell cycle exit, it is currently unclear whether the effects of pRb on differentiation are an indirect consequence of pRb/E2F-mediated cell cycle control or whether they reflect direct cell-type-specific pRb functions. We have mutated *Rb1* in the mouse to express a protein (R654W) specifically deficient in binding E2F1, E2F2, and E2F3. R654W mutant embryos exhibit cell cycle defects the same as those of *Rb1* null embryos, reinforcing the importance of the interactions of pRb with E2F1, E2F2, and E2F3 for cell cycle control. However, R654W embryos survive at least 2 days longer than *Rb1* null embryos, and increased life span is associated with improved erythrocyte and fetal liver macrophage differentiation. In contrast, R654W pRb does not rescue differentiation defects associated with pRb-deficient retinae. These data indicate that *Rb1* makes important cell-type-specific contributions to cellular differentiation that are genetically separable from its general ability to stably bind E2F1, E2F2, and E2F3 and regulate the cell cycle.**

The *Rb1* tumor suppressor gene is essential for embryonic development, as nullizygous mice die in midgestation (6, 22, 25). Nullizygous embryos exhibit developmental defects in the eye, brain, peripheral nervous system, muscle, liver, placenta, and hematopoietic system, among other defects (21, 45, 48, 51). Unscheduled cell proliferation is frequently observed in a number of these tissues, consistent with the well-characterized ability of *Rb1* protein (pRb) to restrain the cell cycle (17). *Rb1* protein binds and regulates members of the E2F family of transcription factors (9); four E2F family members, the transcriptional activators E2F1, E2F2, and E2F3 and the transcriptional repressor E2F4, normally associate with pRb (11). Binding of pRb blocks E2F-mediated transcriptional activation and facilitates active gene silencing by recruitment of chromatin-modifying factors to promoters containing E2F binding sites. Since E2F activity regulates many cell cycle genes and is required for a normal cell cycle (52), repression of E2F-dependent transcription is generally considered the principal mechanism underlying pRb-mediated cell cycle control.

Rb1 loss also compromises cell-type-specific fate determination and differentiation (8). The ability of pRb to bind and modulate the activity of tissue-specific transcription factors has been proposed to be the mechanism responsible for these effects on differentiation (21, 32, 47). Since differentiation is tightly coupled to cell cycle exit, however, it is also possible that pRb facilitates differentiation indirectly by restraining the cell cycle. Hence, a major challenge is determining whether pRb's effects on differentiation reflect direct, cell-type-specific mechanisms or whether they are an indirect consequence of pRb-mediated cell cycle regulation. Evidence from *Rb1* null mouse retinae indicates there is only mild deregulation of retinal progenitor cell proliferation but a dramatic reduction in mature rod photoreceptors (12, 13, 30, 41, 43, 53). Lineage and gene expression analysis suggests that the role of pRb in rod photoreceptor differentiation is distinct from its role in retinal progenitor cell proliferation (53). The differentiation of fetal liver macrophages (FLM) and myoblasts also defective in the absence of *Rb1*. These defects may be distinct from pRb/E2F-mediated cell cycle control, as they are partially rescued by the compound loss of *Id2* or N-*ras*, respectively (21, 46). Although such genetic studies support a direct role for *Rb1* in cellular differentiation, they cannot exclude possible influences of pRb-mediated cell cycle regulation on differentiation since they utilize null *Rb1* alleles.

To address this issue, we have generated a mutant *Rb1* allele in the mouse that encodes a protein with an arginine-to-tryptophan substitution at codon 654 (R654W). This mutation is analogous to the naturally occurring human R661W *Rb1* mutation associated with partially penetrant, hereditary retinoblastoma (28, 36). The R661W mutation belongs to a class of partially penetrant mutations that introduce changes in the primary amino acid sequence without affecting mRNA or protein expression (18). R661W pRb is unable to physically or functionally interact with E2F (37, 38, 44, 49). In vitro assays indicate R661W is defective for cell cycle control and yet

* Corresponding author. Mailing address: Department of Pharmacology & Therapeutics, Roswell Park Cancer Institute, Elm & Carlton Streets, Buffalo, NY 14263. Phone: (716) 845-4506. Fax: (716) 845-8857. E-mail: david.goodrich@roswellpark.org.

† Supplemental material for this article may be found at http://mcb.asm.org/.

‡ These authors contributed equally to the work.

retains some activity to promote cellular differentiation (44). Presumably, such residual functions account for the decreased penetrance and expressivity observed in hereditary retinoblastoma families carrying the allele. Phenotypic analysis of mice carrying the analogous R654W allele should allow the identification of cell-type-specific, pRb-dependent in vivo functions that are genetically separable from pRb/E2F-mediated cell cycle control.

MATERIALS AND METHODS

Generation the R654W *Rb1* mouse allele. The homology arms used in the targeting vector were PCR amplified from a 129/SV murine *Rb1* bacterial artificial chromosome clone. Codon 654 in exon 20 of the targeting vector was mutated using the QuikChange method according to the manufacturer's recommendations (Stratagene, La Jolla, CA). Exons and flanking intronic regions were verified by DNA sequencing. A 3′-flanking probe was used to screen 158 G418-resistant embryonic stem (ES) cell clones by Southern blotting of BamHI-restricted genomic DNA. Targeting was verified by Southern blotting of EcoRI-restricted genomic DNA using a 5′-flanking probe. A *neo* probe was used to verify that each clone contained a single copy of the targeting construct.

Germ line-transmitting chimeras were generated from two targeted ES cell clones. Chimeras were mated to Zp3-*cre* mice to remove the floxed *neo* selection cassette, and agouti offspring were genotyped by Southern blotting of tail DNA using the 5′-flanking probe. Routine genotyping was performed by PCR amplification of tail DNA by using the primers 5′GGTCACTTGAATGTGATATAT AGC3′, 5′GCTATACGAAGTTATATCG3′, and 5′TATGGAATGCTGCTA ATAC3′.

Reporter gene assay. The murine wild-type *Rb1* expression plasmid is pECE-ΔB/X-HA, which was kindly provided by Brenda Gallie (University of Toronto). The substitution mutants were constructed by site-directed mutagenesis of the parent plasmid using the QuikChange method. The coding region of the expression plasmids was verified by DNA sequencing. C33A cells were obtained from ATCC and cultured in Dulbecco's modified Eagle's medium (BioWhittaker, Maryland) supplemented with 10% fetal bovine serum and antibiotics. The reporter gene assay was performed using an E2F1 promoter luciferase reporter plasmid and the E2F1 expression plasmid (34). A *Renilla* luciferase-expressing plasmid was used to normalize for transfection efficiency. These plasmids were transfected along with the *Rb1*-expressing plasmids into C33A cells by use of Lipofectamine (Invitrogen, Carlsbad, CA) according to the manufacturer's recommendation. Two days after transfection, cells were assayed for firefly and *Renilla* luciferase activity by use of a dual luciferase reporter assay system (Promega, Madison, WI).

Fatty acid analysis. Tissues were homogenized in chloroform-methanol (2:1, vol/vol), and lipids were extracted as described previously (16). Individual lipid classes were separated by thin-layer chromatography using silica gel 60-Å plates developed in petroleum ether, ethyl ether, acetic acid (80:20:1) and visualized by use of rhodamine 6G. Phospholipids and triglycerides were scraped from the plates and methylated using BF_3-methanol as described previously (33). The methylated fatty acids were extracted and analyzed by gas chromatography. Fatty acid methyl esters were identified by comparing the retention times to those of known standards. The inclusion of lipid standards with odd-chain fatty acids permitted lipid quantitation in the sample.

Cell cycle analysis. The cell cycle distribution of asynchronously growing, early-passage (passage number, <5) mouse embryonic fibroblasts (MEF) was assayed by propidium iodide staining and flow cytometry. Histograms were modeled using Modfit software. For analysis of proliferation at high cell density, cultures were maintained at confluence for 3 days, and then bromodeoxyuridine (BrdU) was added for 15 h. Fixed cells were stained with BrdU antibody (Amersham, Piscataway, NJ) and fluorescein isothiocyanate-conjugated secondary antibody (Sigma, St. Louis, MO). For analysis of DNA damage response, subconfluent cultures were treated with 20 Gy γ radiation or cisplatin at 16 μM. Fourteen hours later, BrdU was added, and incubation was continued for an additional 10 h before fixing and staining were done.

Protein analysis and histology. Multiple isolates of early-passage and late-passage (passage number, >25) MEF were extracted and protein lysates immunoprecipitated as previously described (27). E2F and Id2 antibodies were from Santa Cruz Biotechnology (E2F1, Sc-193; E2F2, Sc-633; E2F3, Sc-878; E2F4, Sc-1082; Id2, Sc-489). *Rb1* protein captured in the immunoprecipitates was detected by Western blotting using the antibody G3-245 (Pharmingen, San Diego, CA). The same antibodies were used to measure input levels of E2F, Id2, or *Rb1* protein in extracts by Western blotting. Hsp70 (SPA-820; Stressgen, Victoria, BC, Canada) or β-actin (CP01; Oncogene Research Products, San Diego, CA) antibody staining served as loading controls.

Peripheral blood samples were obtained from umbilical cords, and smear samples were stained with Wright-Giemsa solution (Sigma, St. Louis, MO). Embryos were fixed in 10% formalin and embedded, and 5-μm sections were cut and stained with hematoxylin and eosin. The antibodies used for immunohistocytochemistry were F4/80 (A3-1), TER119 (both from Caltag Laboratories, Burlingame, CA), phospho-histone H3 (06-570; Upstate, Waltham, MA), and activated caspase-3 (9661; Cell Signaling, Beverly, MA).

Retinal analysis. The conditional, floxed allele of *Rb1* was described previously (31). Cre-mediated excision from the floxed *Rb1* allele in retinae was verified by PCR amplification of predicted recombination junction fragments (see Fig. S1B in the supplemental material). Possible Cre-mediated interchromosomal recombination between the floxed and R654W *Rb1* alleles was not detected in genomic DNA from *Chx10-cre*; $Rb1^{Lox/654}$ retinae by PCR amplification of the predicted recombination junctions. Hence, the phenotypes observed in *chx10-cre*; $Rb1^{Lox/654}$ retinae were due to hemizygosity of the R654W allele.

Retinae from P14 pups were immunostained with antibodies to the major classes of retinal cell types (see Table S1 in the supplemental material). Retinal cryosections and dissociated retinae were immunolabeled as described previously (14, 15). To label S-phase retinal progenitor cells, freshly dissected retinae were incubated in 1 ml explant culture medium containing [^{3}H]thymidine (5 μCi ml^{-1}; 89 Ci mmol^{-1}) or 10 μM BrdU for 1 h at 37°C. Autoradiography and BrdU detection were carried out as described previously (14, 15). For apoptosis analysis, a colorimetric terminal deoxynucleotidyltransferase-mediated dUTP-biotin nick end labeling apoptosis system (Promega, Madison, WI) was used, with tyramide-Cy3 being used for detection. Real-time PCR was performed using an ABI 7900 HT sequence detection system (Applied Biosystems, Foster City, CA). Primers and probes were designed using Primer Express software. Probes were synthesized with 5′-labeled 6-carboxyfluorescein and 3′-labeled BMQ. RNA was prepared using Trizol, and cDNA was synthesized using a Superscript system (Invitrogen, Carlsbad, CA). Samples were analyzed in duplicate and normalized to glyceraldehyde-3-phosphate dehydrogenase and GPI1 expression levels.

RESULTS

Construction of the R654W *Rb1* allele. We used targeted homologous recombination in murine ES cells to generate a knock-in *Rb1* allele containing the R654W mutation. The targeting vector contained a 5.1-kbp fragment of the murine *Rb1* gene spanning exons 19 and 20 with a floxed *neo* selection cassette inserted into intron 19 (Fig. 1A). The CGA at codon 654 in exon 20 was mutated to TGG in the targeting vector. Upon the removal of the *neo* selection cassette, the targeted allele contained the R654W mutation and a single *loxP* site in place of 86 bp of normal intron 19 sequence. Five correctly targeted ES cell clones were obtained, as assessed by Southern blotting using a 5′-flanking probe. Two ES cell clones were used to create germ line-transmitting chimeras. These chimeras were crossed with Zp3-*cre* mice to remove the drug selection cassette. The predicted structure of the targeted allele was confirmed by Southern blotting using 5′- and 3′-flanking probes (Fig. 1B). A PCR assay that distinguished between the wild-type and mutant alleles was used for routine genotyping (Fig. 1C).

The two resulting mouse strains heterozygous for the R654W mutation were fertile and apparently normal. The strains were maintained on a mixed genetic background (C57BL/6 × 129/Sv). Both exhibited the same highly penetrant phenotype during subsequent analysis; hence, data from each strain were not further distinguished. RNA from the carcasses of postcoitum day 14.5 (E14.5) embryos was analyzed by reverse transcription-PCR (RT-PCR) and DNA sequencing to validate expression of the mutant allele (Fig. 1D). Heterozygous embryos expressed both the wild-type (CGA) and mu-

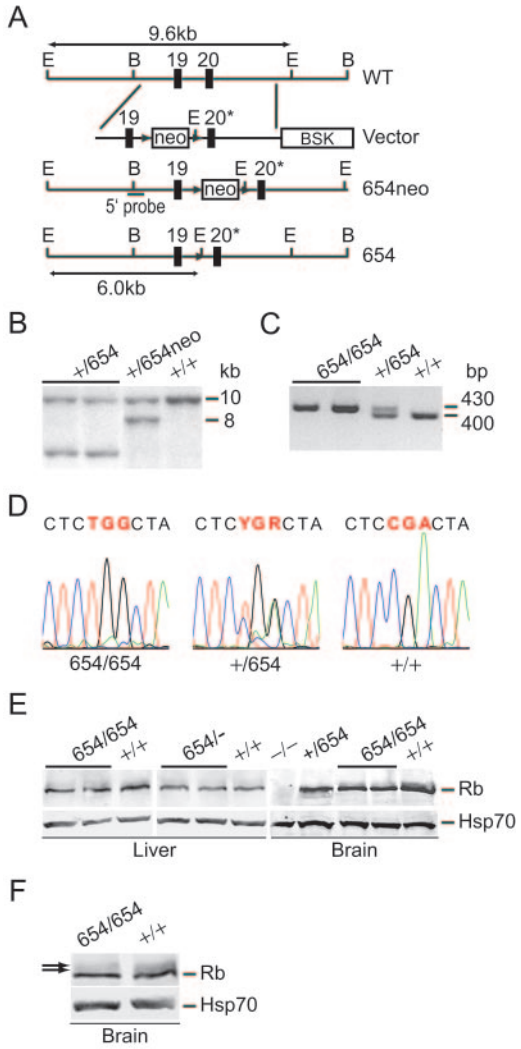

FIG. 1. Generation of R654W *Rb1* mutant mice. (A) Representation of the exon/intron structure of the *Rb1* gene, the targeting vector, and the expected structures of the successfully targeted allele. Exons are numbered and shown as solid boxes. The positions of the restriction enzyme sites (E, EcoRI; B, BamHI) and the 5′-flanking probe and the expected sizes of fragments detected by Southern blotting are indicated. (B) Southern blot analysis of representative mice with the indicated genotypes using the 5′-flanking probe and EcoRI-restricted genomic DNA. (C) PCR genotyping of mice. The targeted allele lacking the *neo* selection cassette generates a 430-bp band, while the wild-type allele amplifies a 400-bp band. (D) RNA from embryos of the indicated genotypes was amplified by RT-PCR. PCR fragments were sequenced, and representative chromatograms spanning the region of codon 654 are shown. The DNA sequence indicated by the chromatogram is listed above, with the codon 654 triplet highlighted. (E) Liver and brain protein extracts from E13.5 embryos of the indicated genotypes were analyzed by Western blotting with an antibody directed against pRb. Hsp70 served as a loading control. (F) Brain protein extracts from E13.5 embryos of the indicated genotypes were analyzed for pRb phosphorylation by Western blotting. Note the presence of pRb species with reduced electrophoretic mobility that are characteristic of hyperphosphorylated pRb. Hsp70 served as a loading control.

tant (TGG) RNA in roughly equal quantities. *Rb1* protein levels in the brains and livers of homozygous, heterozygous, hemizygous (654/−), or wild-type embryos were approximately equal, as assessed by Western blotting (Fig. 1E). Hence, the mutant allele was expressed at a level comparable to that of the wild-type allele. Specimens of *Rb1* protein from brain extracts of both wild-type and homozygous R654W mice show evidence of phosphorylation, as indicated by the presence of slower-migrating forms of the protein that are characteristic of hyperphosphorylation (Fig. 1F). While additional analysis would be required to assess whether the levels of site-specific phosphorylation of wild-type and mutant proteins are similar, the data suggest that R654W pRb can be phosphorylated, which is in agreement with results from previous studies of the analogous human R661W mutant (37).

R654W pRb is deficient in binding E2F1, E2F2, and E2F3 and regulating the cell cycle. To test the ability of wild-type and R654W pRb to associate with E2F, we analyzed total protein extracts from MEF of the relevant genotypes by coimmunoprecipitation. E2F1, E2F2, and E2F3 immunoprecipitates capture 10- to 20-fold less pRb from homozygous R654W MEF extracts than from wild-type extracts, based on the quantitation of relative signal levels from multiple blots (Fig. 2A). Input levels of E2F1 and E2F3 are noticeably higher in R654W MEF extracts than in wild-type extracts (Fig. 2A, right panel), so the coimmunoprecipitation results may overestimate the avidity of R654W pRb/E2F1 or pRb/E2F3 binding. Since E2F1 and E2F3 are themselves E2F regulated, this observation also indicates that any residual R654W pRb/E2F binding is unable to normally regulate E2F1 or E2F3 expression. The inability of R654W pRb to functionally interact with E2F1 has been confirmed by use of a sensitive reporter gene assay (Fig. 2B). Exogenously expressed wild-type pRb efficiently represses expression from a reporter gene driven by the E2F-responsive E2F1 promoter. In contrast, R654W pRb demonstrates no activity in this assay relative to the empty vector control or a previously characterized null pRb mutant (C706Y). As expected, the analogous human mutant (R661W) also fails to show significant activity in this assay, consistent with previously published data (1, 37, 44).

Surprisingly, immunoprecipitates of the repressor E2F4 typically capture more pRb from homozygous R654W MEF extracts than from wild-type extracts. Increased association of R654W pRb with E2F4 in the absence of stable interaction with activating E2Fs is reproducible in multiple isolates of MEF as well as in liver extracts of the relevant genotypes, indicating that the pattern of E2F binding is not cell line or cell type specific (data not shown). Since R654W pRb retains the ability to stably bind E2F4, the R654W mutation does not cause a general decrease in protein binding activity; rather, it affects some protein interactions but not others. The data also indicate that pRb binds to E2F1, E2F2, and E2F3 in a manner that is biochemically distinguishable from the way in which it binds E2F4.

Previous reports demonstrated various cell cycle defects in *Rb1* null MEF cultured in vitro. For example, loss of *Rb1* caused a shift in cell cycle distribution in asynchronously growing MEF and compromised their ability to arrest at G_1/S in response to DNA damage (19). Loss of *Rb1* also compromised confluence-induced cell cycle arrest of MEF (24). We compared *Rb1* null and R654W MEF in these aspects of in vitro cell cycle control. Relative to asynchronous cultures of wild-type MEF, both *Rb1* null and homozygous R654W MEF had an increased fraction of cells in the S and G_2/M phases of the

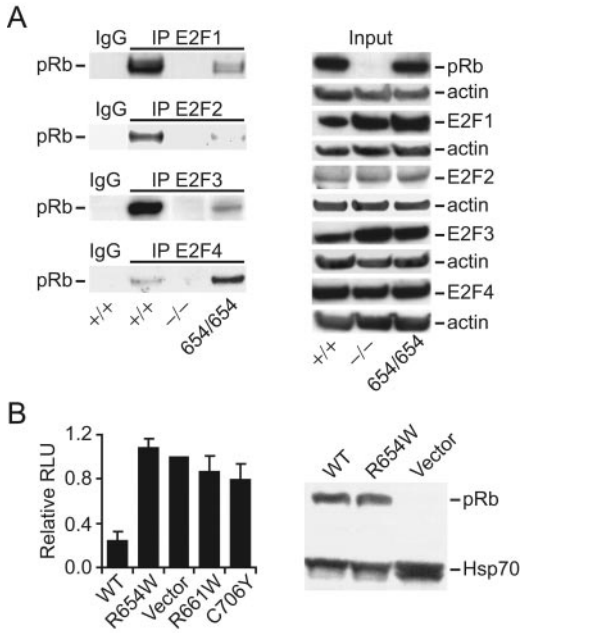

FIG. 2. R654W pRb is deficient in E2F1, E2F2, and E2F3 binding and transcriptional regulation. (A) MEF extracts of the indicated genotypes were immunoprecipitated (IP) with antibodies directed against the E2F proteins shown or with nonspecific immunoglobulin G (IgG) as a negative control. The level of pRb coimmunoprecipitating with E2Fs was determined by Western blotting. The panels at right show the input levels of E2Fs and pRb. β-Actin served as a loading control. (B) Expression vectors designed to express wild-type (WT) or R654W murine pRb or previously characterized human R661W or C706Y pRb were transfected into C33A cells with an E2F1 promoter luciferase reporter gene and an E2F1 expression plasmid. Extracts from transfected cells were assayed for luciferase activity. Firefly luciferase light units (RLU) were background subtracted, corrected for variation in transfection efficiency, and normalized to the vector control. The data represent the means and standard deviations from three experiments done in duplicate. Note that R654W pRb, like the analogous human R661W mutant, has no detectable ability to repress E2F1-dependent transcription relative to the vector control or a pRb null mutant (C706Y). The panel at right shows a Western blot indicating the levels of ectopic murine pRb expression observed in the transfections. Hsp70 served as a loading control.

cell cycle (Fig. 3A). *Rb1* null and R654W MEF cultured at confluence also had equally high percentages of cells incorporating BrdU in S phase. In contrast, a low percentage of wild-type MEF incorporated BrdU when cultured at confluence (Fig. 3B). Finally, *Rb1* null and R654W MEF failed to efficiently trigger G_1/S cell cycle arrest in response to DNA damage. In contrast to wild-type MEF, both *Rb1* null and R654W MEF exhibited large fractions of BrdU-positive cells subsequent to treatment by irradiation or with cisplatin (Fig. 3C).

Loss of *Rb1* also leads to a detectable cell cycle deregulation in vivo, as *Rb1* null mice exhibit unscheduled cell proliferation in the eye lens and the nervous system. This loss of cell cycle control is associated with increased apoptosis. To test whether R654W embryos show a similar loss of cell cycle control in vivo, tissue sections were stained for phosphorylated histone H3 to mark proliferating mitotic cells or for activated caspase 3 to mark apoptotic cells. Ectopic mitoses and apoptosis are readily detected in the lens fiber compartment of eyes from

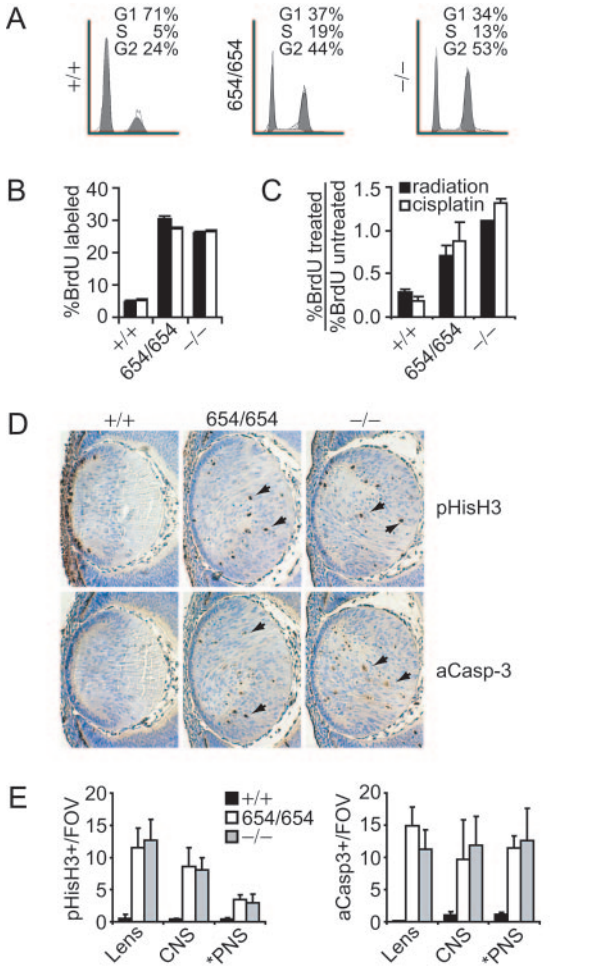

FIG. 3. R654W pRb is deficient in cell cycle control in vitro and in vivo. (A) The cell cycle distributions of asynchronously growing MEF were determined by propidium iodide staining and flow cytometry. A representative histogram is shown. (B) MEF were cultured at confluence and the fractions of proliferating cells counted by BrdU incorporation. The black and white bars represent two independent MEF isolates. The data are the means and standard deviations from two independent experiments done in triplicate. In some cases, the error bars may be too small to see, given the scale of the graph. (C) Asynchronously growing MEF were treated with ionizing radiation or cisplatin. The fractions of cells incorporating BrdU, relative to that of untreated controls, were calculated. The data shown are the means and standard deviations from two independent experiments performed in triplicate. (D) Transverse sections of the eye from E13.5 embryos were stained for phosphorylated histone-H3 (pHisH3) or activated caspase 3 (aCasp-3). Arrows indicate positively stained cells in the lens fiber compartment. Note that the lens fiber cells are disorganized in the mutant embryos relative to those in the wild-type embryos. (E) Ectopic cell proliferation and apoptosis were quantitated in the eye lens, the intermediate zone of the fourth ventricle (central nervous system [CNS]), and the trigeminal ganglia (peripheral nervous system [PNS]) as the number of stained cells per microscopic field of view (FOV) at ×630 magnification. The data represent the mean and standard deviation from at least four embryos, counting three nonconsecutive sections per embryo. Differences between wild-type and either of the mutant *Rb1* embryos were statistically significant ($P \leq 0.01$). *, the peripheral nervous system values are divided by 10.

both *Rb1* null and R654W E13.5 embryos but not in that from wild-type embryos (Fig. 3D). This cell cycle deregulation probably contributes to the disorganization of the lens fiber cells in the mutant embryos; note that the nuclei of lens fiber cells are organized along the midline of the lens of wild-type embryos, but that this is not so for mutant embryos. Ectopic mitosis and apoptosis are also detected in the central nervous system (intermediate zones of the third and fourth ventricles) and the peripheral nervous system (trigeminal and dorsal root ganglia) of both R654W and *Rb1* null embryos. The numbers of mitotic or apoptotic cells detected per unit area are similar in both *Rb1* null and R654W embryos for all tissues examined (Fig. 3E). Since in vivo and in vitro cell cycle defects are similar in terms of cells expressing R654W pRb and in terms of cells completely lacking pRb, R654W pRb does not have a detectable ability to enforce cell cycle control within the biological contexts examined.

R654W pRb partially rescues developmental defects characteristic of *Rb1* null embryos. Intermating of heterozygous R654W mice failed to yield viable offspring homozygous for the R654W allele from among the more than 340 pups that were genotyped. Hence, the R654W allele was insufficient to support normal embryonic development. We assessed embryo cardiac function as a measure of viability from gestational ages E13.5 to E18.5 to compare the timings of lethality in *Rb1* null and R654W homozygous embryos. Consistent with previously published reports (6, 22, 25), live *Rb1* null embryos were rarely recovered at E15.5 (2 of 11 viable) and were never recovered at E16.5 or later (0 of 7 viable). In contrast, live homozygous R654W embryos were routinely recovered at E15.5 (11 of 18 viable) and E16.5 (6 of 11 viable). Live homozygous R654W embryos could be recovered as late as E17.5 (2 of 18 viable). R654W allele dosage did not have a significant effect on viability, since hemizygous R654W embryos (654/−) survived at least as long as homozygous R654W embryos (16 of 18 viable at E15.5 and 3 of 7 viable at E17.5). On average, embryos homozygous for R654W *Rb1* survived at least 2 days longer than *Rb1* null embryos.

Homozygous or hemizygous R654W embryos exhibit gross morphological defects that are similar to those of *Rb1* null embryos although generally less severe (Fig. 4A). For example, *Rb1* null embryos are considerably smaller than wild-type littermates and exhibit pale coloration. Homozygous or hemizygous R654W embryos are larger than age-matched *Rb1* null embryos and exhibit improved coloration. The pale color of *Rb1* null embryos has been associated with deficient erythrocyte maturation (6, 22, 25). To assess erythrocyte maturation in R654W embryos, we counted the percentage of mature, enucleated erythrocytes in peripheral blood at different stages of gestation. The percentage of enucleated erythrocytes is significantly greater in the blood of homozygous or hemizygous R654W embryos than in that of *Rb1* null embryos. At later stages of gestation, the percentage of enucleated erythrocytes approaches 90%, close to the percentage observed in wild-type embryos (Fig. 4B). A small percentage of erythrocytes still exhibit enucleation defects and other morphological abnormalities in E17.5 homozygous or hemizygous R654W embryos (Fig. 4C). Hence, the R654W allele partially rescues the erythrocyte maturation defect associated with the complete loss of *Rb1*.

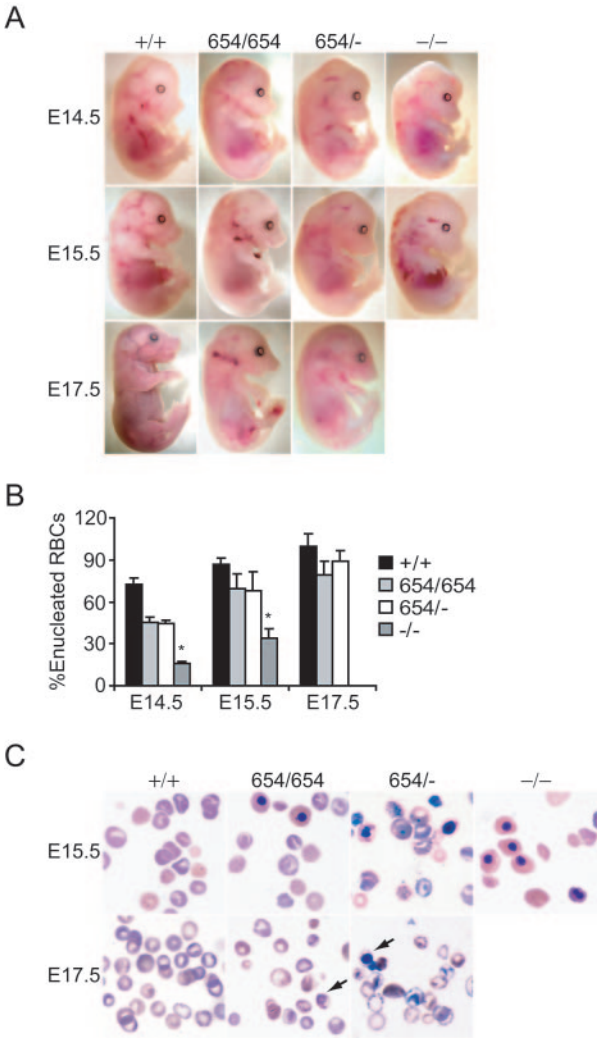

FIG. 4. Improved erythrocyte maturation in R654W embryos. (A) Embryos of the indicated gestational ages and genotypes were photographed in saline. (B) The percentages of enucleated erythrocytes (RBCs) were determined for peripheral blood smear samples. The data points represent the means and standard deviations from at least three embryos. (C) Photographs of representative Wright-Giemsa-stained peripheral blood smears at later stages of gestation. Arrows show examples of the residual enucleation defects that occurred in a small percentage of erythrocytes in E17.5 R654W embryos. ∗, significant difference ($P < 0.01$) between *Rb1* null and R654W embryos.

Rb1 can affect erythrocyte differentiation through both cell-intrinsic and cell-extrinsic mechanisms (5, 29, 29, 45, 45, 50, 50). Defective placental transport caused by unscheduled proliferation of labyrinth trophoblasts in the absence of pRb is one such cell-extrinsic mechanism (51). We have examined placental transport function to determine if it accounts for improved erythrocyte maturation and survival of R654W embryos. Placental transport can be quantitated by measuring the accumulation of essential fatty acids (EFA) in the fetus relative to the levels supplied to the placenta by the mother. Since EFA are obtained only from the diet, EFA accumulation in the fetus is proportional to placental transport. Consistent with previously published data (51), *Rb1* null E14.5 fetuses show a 7.2%

TABLE 1. Essential fatty acid transport in *Rb1* mutant embryos

Sample	% of total fatty acid composition	
	18:02 + 20:04 + 22:06[a]	16:0 + 18:0[b]
Wild type (n = 9)		
Placenta	40.2 ± 1.5	43.2 ± 1.3
Fetus	30.6 ± 0.9	42.8 ± 0.4
Ratio of fetus/placenta	0.76 ± .02	0.99 ± .04
654/654 (n = 5)		
Placenta	40.5 ± 1.2	42.9 ± 1.0
Fetus	28.5 ± 1.0	42.1 ± 0.7
Ratio of fetus/placenta	0.70 ± .02	0.98 ± .01
% Reduction[c]	7.7[d]	1.1[e]
−/− (n = 4)		
Placenta	40.4 ± 2.0	42.1 ± 0.3
Fetus	28.5 ± 1.1	43.8 ± 2.0
Ratio of fetus/placenta	0.71 ± .03	1.04 ± .07
% Reduction[c]	7.2[d]	−4.8[e]

[a] Essential fatty acids.
[b] Nonessential fatty acids.
[c] Reduction in fetal fatty acid accumulation compared to that for the wild type (% for wild-type fetus − % for mutant fetus/% for wild-type fetus normalized for placental fatty acid accumulation).
[d] $P \leq 0.01$ by Student's t test.
[e] $P > 0.1$ by Student's t test.

($P < 0.01$) reduction in accumulation of the EFA linoleic acid (18:02), arachidonic acid (20:04), and docosahexaenoic acid (22:06) relative to the level seen in wild-type fetuses (Table 1). Homozygous R654W fetuses show a similar 7.7% reduction ($P < 0.01$). As expected, no statistically significant difference is observed in the fetal accumulations of the nonessential fatty acids palmitic acid (16:0) and stearic acid (18:0), since these are produced in the fetus and do not require placental transport. Disruptions of normal labyrinth architecture are also similar in both *Rb1* null and R654W E13.5 placentae (Fig. 5A). In particular, the porous appearance of the labyrinth layer characteristic of a wild-type placenta is absent in both *Rb1* null and homozygous R654W placentae. The reduced surface area of the blood spaces within the labyrinth layer probably contributes to the placental transport defect (51). Since R654W and *Rb1* null embryos exhibit quantitatively similar placental transport defects, placental transport is unlikely to account for improved erythrocyte maturation in R654W embryos.

In the absence of *Rb1*, FLM show defects in differentiation, as reflected by their smaller size, lack of extensive cytoplasmic projections, and weak staining for the mature macrophage marker F4/80. As a consequence, TER119-positive erythroid cells fail to associate normally with these defective FLM in erythroblastic islands, thereby compromising erythrocyte maturation (21). Compared to *Rb1* null livers, FLM in homozygous R654W livers show improved differentiation, as indicated by the presence of larger cytoplasmic projections on F4/80-positive FLM and a higher density of F4/80-positive FLM per unit area of the liver (Fig. 5B and C). In addition, the fraction of F4/80-positive FLM in close association with five or more TER119-positive erythroid cells is significantly greater in homozygous R654W livers than in *Rb1* null livers, suggesting an improvement in the formation of erythroblastic islands. Although phenotypic rescue by R654W pRb is incomplete, as

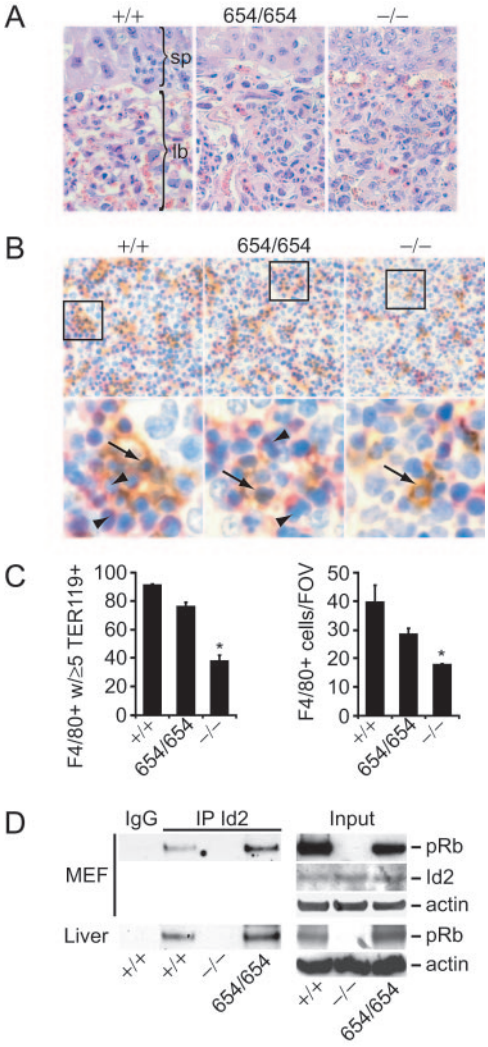

FIG. 5. Effects of R654W pRb on the placenta and FLM differentiation. (A) Hematoxylin-and-eosin-stained sections of E13.5 placentae are shown. sp, spongiotrophoblast layer; lb, labyrinth. (B) E14.5 liver sections were stained for F4/80 (brown) and TER119 (pink). The squares show the regions of the images magnified in the lower panels. Arrows indicate F4/80-positive FLM, while arrowheads designate some of the TER119-positive cells associated with FLM in erythroblastic islands. Note the lack of extensive cytoplasmic projections of *Rb1* null FLM and the relative dearth of associated TER119-positive cells. (C) The percentages of F4/80-positive cells associated with ≥5 TER119-positive cells and the densities of prominently stained F4/80-positive cells per microscopic field of view (FOV) in liver sections are shown. The data points represent the means and standard deviations for at least three embryos, counting three nonconsecutive sections per embryo. *, significant difference between R654W and *Rb1* null livers ($P < 0.01$). (D) MEF or liver tissue extracts of the indicated genotypes were immunoprecipitated with Id2 antibody or an immunoglobulin G (IgG) control. The immunoprecipitates were analyzed for the presence of pRb by Western blotting. The relative input levels of pRb and Id2 were determined by Western blotting (panels at right). β-Actin served as a loading control.

the density of FLM and their association with TER119-positive erythroid cells is still lower than in wild-type livers, these observations suggest that R654W pRb retains some capacity to promote FLM differentiation.

Id2 is an inhibitor of the tissue-restricted transcription factor

TABLE 2. Ectopic proliferation and cell type distribution in P14 $Rb1^{654/-}$ retinae[a]

Cell type[b]	Ectopic proliferation, cell type distribution[c] in the retinae of individual mice of the indicated genotype			
	Chx10-cre; $Rb1^{654/+}$	*Chx10-cre*; $Rb1^{+/-}$	*Chx10-cre*; $Rb1^{Lox/654}$	*Chx10-cre*; $Rb1^{Lox/654}$
$BrdU^+$	>0/250, 0/250 (0)	0/250, 0/250 (0)	5/250, 4/250 (1.8 ± 0.3)	11/250, 6/250 (3.4 ± 1.4)
$Rhod^+$	145/250, 130/250 (55 ± 4.2)	151/250, 122/250 (54 ± 8.2)	65/250, 55/250 (24 ± 2.8)	78/250, 69/250 (29 ± 2.5)
$Recov^+$	139/250, 127/250 (53 ± 3.3)	168/250, 150/250 (64 ± 5.1)	64/250, 68/250 (26 ± 1.1)	23/250, 27/250 (10 ± 1.1)
$Cone^+$	6/250, 4/250 (2 ± 0.5)	7/250, 4/250 (2.2 ± 0.8)	7/250, 5/250 (2.4 ± 0.5)	6/250, 7/250 (2.6 ± 0.2)
$PKC\alpha^+$	10/250, 9/250 (3.8 ± 0.3)	8/250, 6/250 (2.8 ± 0.5)	8/250, 11/250 (3.8 ± 0.8)	10/250, 9/250 (3.8 ± 0.2)
$Chx10^+$	19/250, 17/250 (7.2 ± 0.5)	12/250, 16/250 (5.6 ± 1.1)	27/250, 22/250 (9.8 ± 1.4)	32/250, 28/250 (12 ± 1.1)
$Pax6^+$	11/250, 9/250 (4 ± 0.5)	6/250, 8/250 (2.8 ± 0.5)	24/250, 23/250 (9.4 ± 0.2); **16% ± 2%**[d]	23/250, 20/250 (8.6 ± 0.8); **12% ± 3%**[d]
$Syntax^+$	20/250, 18/250 (7.6 ± 0.5)	14/250, 11/250 (5 ± 0.8)	11/250, 9/250 (4 ± 0.5)	5/250, 7/250 (2.4 ± 0.5)
$Calb^+$	1/500, 2/500 (0.3 ± 0.1)	1/500, 0/500 (0.1 ± 0.1)	1/500, 0/500 (0.1 ± 0.1)	1/500, 0/500 (0.1 ± 0.1)
$GluSyn^+$	4/250, 5/250 (1.8 ± 0.3)	5/250, 6/250 (2.2 ± 0.3)	17/250, 13/250 (6.0 ± 1)	22/250, 27/250 (9.8 ± 0.1.4)

[a] Mice received an intraperitoneal injection of [^{3}H]thymidine (5 μCi/g) 1 hour prior to retinal dissection. [^{3}H]thymidine$^+$ cells expressed Chx10 (~1 to 2% [^{3}H]thymidine$^+$, immunopositive/[^{3}H]thymidine$^+$) and Pax6.

[b] Rhod, rhodopsin; recov, recovesin; PKCα, protein kinase C α; calb, calbindin; GluSyn, glutamine synthetase; syntax, syntaxin; cone, cone arrestin.

[c] Indicated cell type/total (% mean ± % standard deviation).

[d] The fraction of proliferating cells expressing Pax6 ([^{3}H]thymidine$^+$, immunopositive/[^{3}H]thymidine$^+$) is indicated. The number of grains for 10 randomly selected [^{3}H]thymidine-labeled cells varied from 10 to 27 grains per cell (mean, 14 ± 10). The number of grains for 10 randomly selected unlabeled cells varied from 0 to 3.

PU.1, a regulator of macrophage differentiation (35). *Rb1* protein binds Id2 and prevents it from inhibiting PU.1, thereby promoting FLM differentiation (21). We have tested whether this mechanism may account for the improved FLM differentiation observed in R654W embryos. R654W pRb retains the ability to bind Id2, as assessed by coimmunoprecipitation; Id2 immunoprecipitates from MEF or liver extracts capture at least as much R654W pRb as wild-type pRb (Fig. 4D). Hence, the ability to physically interact with Id2 is retained by R654W pRb, and this interaction may directly contribute to the improved differentiation of FLM by blocking Id2-mediated inhibition of PU.1. Further, improved FLM differentiation may indirectly contribute to the increased erythrocyte maturation observed in homozygous R654W embryos.

Retinal defects in homozygous R654W mice. During normal development of the mouse retina, *Rb1* is expressed in proliferating retinal progenitor cells and postmitotic neurons and glia (53). Loss of *Rb1* causes mild deregulation of retinal progenitor cell proliferation, yet there is a dramatic loss of rod photoreceptors. Rather than switching fates, cells destined to become rod photoreceptors remain immature and express retinal progenitor cell markers, such as Pax6 and Chx10. We have examined postnatal retinae to assess the effects of R654W pRb on retinal progenitor cell differentiation. To overcome the embryonic lethality in the mutant mice, we have inactivated a floxed wild-type *Rb1* allele specifically in the retina in a heterozygous R654W background with a *Chx10-cre* transgene. The mating generates offspring heterozygous for the R654W allele, and hence viable, but hemizygous for R654W in retinal cells. Predominant expression of the R654W allele in *Chx10-cre*; $Rb1^{Lox/654}$ retinae has been confirmed by RT-PCR and DNA sequence analysis of RNA (see Fig. S1A in the supplemental material).

Retinae from P14 pups were immunostained with antibodies to the major classes of retinal cell types (see Table S1 in the supplemental material). Rod photoreceptors were significantly reduced in hemizygous R654W retinae, and there were no changes in the quantities of other major cell types (Table 2 and Fig. 6). In particular, cones and bipolar cells differentiated normally (Fig. 6 and Fig. S2 in the supplemental material). Horizontal cell synaptogenesis was also defective in the *Chx10-cre*; $Rb1^{Lox/654}$ retinae, as previously observed in *Rb1* null retinae (12). Proliferating cells incorporating [^{3}H]thymidine expressed markers of retinal progenitor cells, including Chx10 and Pax6. For example, the proportion of Pax6-positive, [^{3}H]thymidine-positive cells to [^{3}H]thymidine-positive cells was 14% ± 2.5% in P14 *Chx10-cre*; $Rb1^{Lox/654}$ retinae (Table 2). No [^{3}H]thymidine-positive cells were detected in the retinae from control littermates (*Chx10-cre*; $Rb1^{654/+}$ or *Chx10-cre*; $Rb1^{+/-}$). Ectopic Pax6- and Chx10-positive cells were observed in the outer nuclear layer, consistent with the observation that cells that normally differentiated into rods remained as immature cells (12, 53). Real-time RT-PCR demonstrated that retinal progenitor cell markers Fgf15, Eya2, and Sfrp1 (2) were upregulated in the *Chx10-cre*; $Rb1^{Lox/654}$ retinae. Expression of the E2F-regulated p107 gene was also upregulated in these retinae, consistent with the lack of pRb/E2F1-, pRb/E2F2-, and pRb/E2F3-mediated transcriptional regulation in these cells. Analysis of E14.5 retinae from homozygous R654W embryos and their heterozygous and wild-type littermates verified that there was no proliferation or differentiation defect in the embryonic retina that could contribute to the failure of rods to form (see Fig. S3 in the supplemental material). In sum, the phenotype of *Chx10-cre*; $Rb1^{Lox/654}$ retinae was indistinguishable from that of *Chx10-cre*; $Rb1^{Lox/-}$ retinae.

DISCUSSION

The data presented here indicate that *Rb1* makes important cell-type-specific contributions to cellular differentiation that are genetically separable from its general ability to stably bind E2F1, E2F2, and E2F3 and regulate the cell cycle. R654W pRb is unable to efficiently bind E2F1, E2F2, and E2F3 and regulate E2F1-, E2F2-, and E2F3-dependent gene expression. As a result, cells expressing R654W pRb are as deficient in several aspects of cell cycle control in vitro and in vivo as cells completely lacking pRb. Compound loss of activating E2Fs has

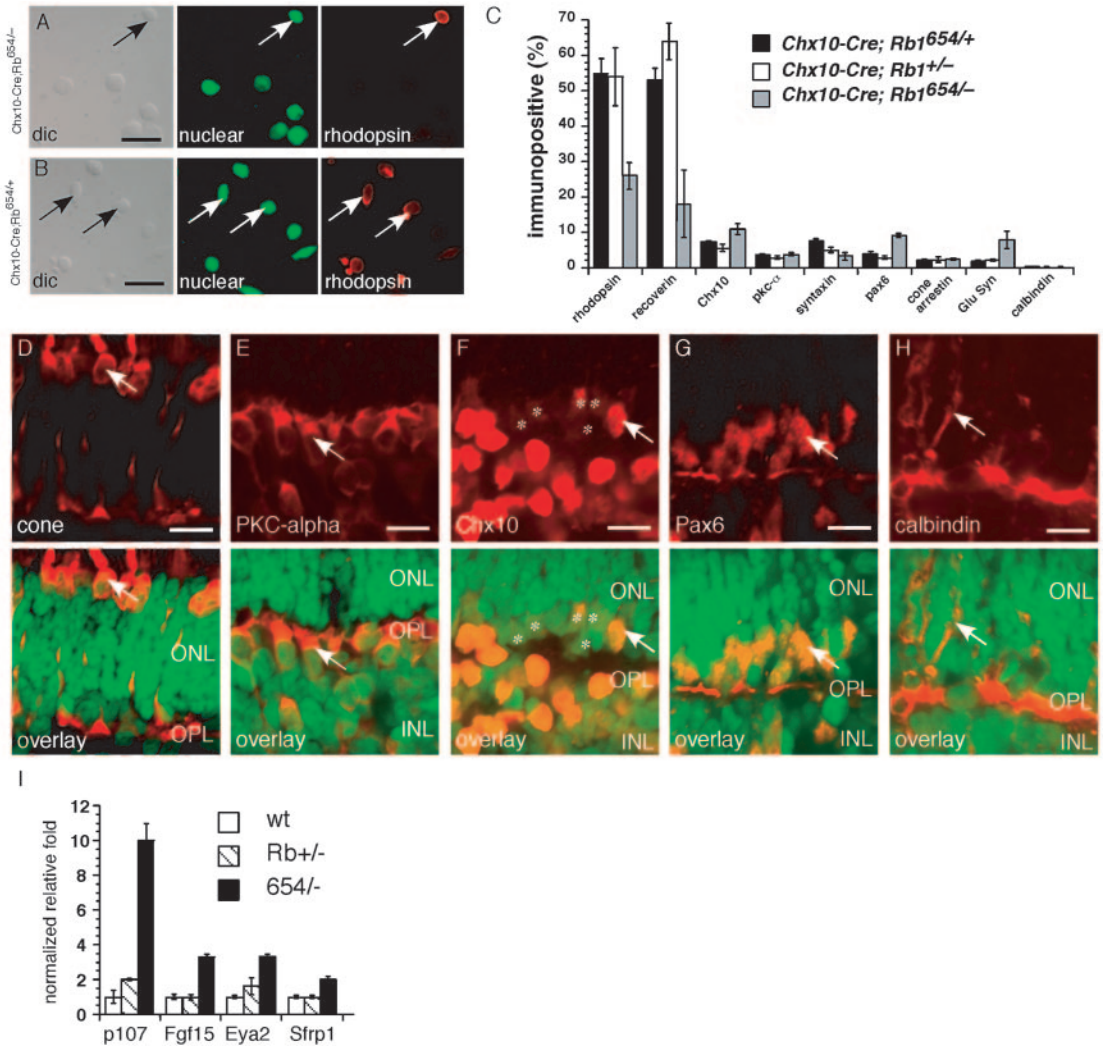

FIG. 6. Effects of R654W pRb on retinal development. (A and B) P14 retinae are immunostained to identify rod cells (arrows). Rod cell defects are produced in a mosaic pattern across the retina due to heterogeneous *Chx10-cre* expression. (C) Quantitation of the proportions of different cell types in dissociated P14 *Chx10-cre*; $Rb1^{Lox/654}$ retinae and in control littermates. (D) Cone photoreceptors are produced in their correct laminar position and proportion (arrow). (E) Protein kinase C α-immunopositive bipolar cells are produced in their correct proportion and position (arrow). (F) Ectopic Chx10-immunopositive cells in the outer nuclear layer are observed (arrow). Many of these ectopic cells are weakly immunopositive (*), suggesting that they are retinal progenitor cells. (G) Ectopic Pax6-immunopositive cells in the outer nuclear layer where rods normally form (arrow). Pax6 is expressed in retinal progenitor cells and mature amacrine cells. (H) Like *Rb1* null retinae, horizontal cells form ectopic processes that extend apically into the outer nuclear layer. (I) Real-time RT-PCR of P14 retinae to assess expression of the genes shown. Abbreviations: ONL, outer nuclear layer; OPL, outer plexiform layer; INL, inner nuclear layer; wt, wild type; PKC-alpha, protein kinase C α; Glu Syn, glutamine synthase; dic, differential interference contrast. Scale bars, 10 μm.

previously shown that the cell cycle defects associated with *Rb1* loss are dependent on activating E2F activity (40, 48, 54), thus establishing E2F1, E2F2, and E2F3 as important targets of pRb-mediated cell cycle control in vivo. The results obtained with R654W pRb extend these findings by demonstrating that genetic interactions between *Rb1* and activating E2Fs are based on direct physical association. Thus, the data provide additional support to the hypothesis that pRb/E2F1, pRb/E2F2, and pRb/E2F3 association is the primary mechanism underlying pRb-mediated cell cycle control. However, the analogous human R661W mutant is also deficient in binding viral oncoproteins containing the LXCXE binding motif (37, 44). Hence, we cannot rule out the possibility that R654W pRb fails to bind other LXCXE-containing cellular proteins that are important for cell cycle regulation. However, disruption of the LXCXE binding domain within pRb does not compromise its ability to enforce cell cycle control (4, 10), so such proteins have yet to be identified.

An E2F-independent mechanism involving pRb/Skp2 interaction and stabilization of p27kip1 has also been proposed to contribute to pRb cell cycle regulation, and human R661W pRb apparently retains this activity (23). We have been able to detect stable pRb/Skp2 interaction in MEF, liver, or rescued prostate epithelial cell extracts, although the R654W pRb typically interacts less well with Skp2 (H. Sun and D. W. Goodrich, unpublished). While pRb/Skp2 binding is detect-

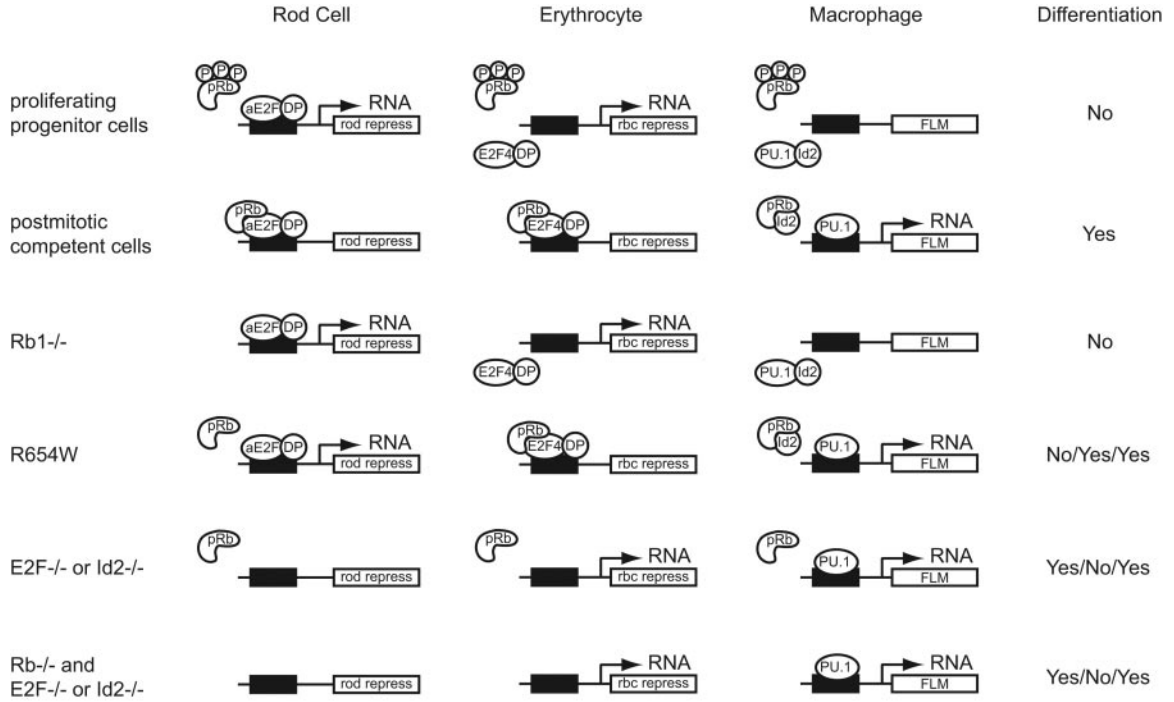

FIG. 7. A model for tissue-specific, pRb-mediated mechanisms in cellular differentiation. In the absence of pRb activity either by protein loss or by inhibitory phosphorylation, the developmental program of retinal cells, erythrocytes, and macrophage progenitor cells is blocked. In retinal progenitors, we propose that this is due to a theoretical retina-specific gene whose expression is dependent on E2F1, E2F2, or E2F3. For erythrocyte progenitors, the theoretical gene is active unless repressed by pRb/E2F4. E2F4 cannot activate gene expression in its free form because it requires association with a pocket protein for nuclear localization. In macrophage progenitors, the activity of the required PU.1 transcription factor is blocked by Id2. In postmitotic, differentiation-competent cells, pRb phosphorylation is reduced and pRb complexes form. Expression of the rod repression gene is blocked by the pRb/E2F1, pRb/E2F2, or pRb/E2F3 complexes, while the red blood cell (rbc) repression gene expression is inhibited by pRb/E2F4. In macrophages, pRb/Id2 interaction blocks Id2 activity, freeing PU.1 to activate expression of the macrophage differentiation program. R654W pRb does not support rod cell differentiation, since it fails to bind E2F1, E2F2, and E2F3. R654W pRb does support erythrocyte and FLM differentiation, due at least in part to the retained pRb/E2F4 and pRb/Id2 interactions. Based on this model, nearly normal rod formation should occur in retinae lacking *Rb1* and E2F1, E2F2, or E2F3, because reduction in E2F activity compromises the expression of the rod repression gene. The loss of Id2 relieves the Id2-mediated block to PU.1 activity, permitting FLM maturation. In contrast, the loss of E2F4 prevents targeting of the pRb/E2F4 repressive complex to the rbc repression gene, thereby blocking erythrocyte maturation. It should be noted that the rod repression gene, the rbc repression gene, and the FLM gene may be a family of genes. Moreover, these genes do not necessarily regulate genes that are directly involved in the differentiation-specific transcriptional network. For example, these regulated genes may alter chromatin structure, a hallmark of rod cell differentiation. DP indicates the heterodimeric binding partners of the E2F transcription factors. aE2F refers to the activating E2F family members E2F1, E2F2, and E2F3. The encircled "P" designates phosphorylation of pRb.

able, the level of p27Kip1 is no greater in wild-type extracts than in *Rb1* null extracts. The pRb/Skp2 mechanism has originally been identified in osteosarcoma cell lines by use of exogenously expressed *Rb1* proteins. Hence, the disparity between our results and those of Ji et al. (23) may be due to the different cell types in which the experiments are performed, differences between human pRb and mouse pRb, or differences in the effects of endogenous versus ectopic pRb expression.

Despite the loss of cell cycle control observed in R654W embryos, embryonic development is partially rescued relative to the development of *Rb1* null embryos. Partial rescue is associated with a significant improvement in the differentiation of some tissues but not of others. Thus, differentiation in these cell types requires a function of pRb that is independent of its general ability to bind E2F1, E2F2, and E2F3 and regulate the cell cycle. We propose a model for three tissue-specific mechanisms that pRb may use to directly influence differentiation (Fig. 7). We suggest that E2F1, E2F2, and E2F3 facilitate expression of a gene that prevents rod cell fate specification in the retina. The pRb/E2F1, pRb/E2F2, and pRb/E2F3 complexes would silence expression of this gene, permitting rod cell differentiation. Previous characterizations of *Rb1* null retinae suggest that impaired rod photoreceptor differentiation is unrelated to progenitor cell cycle control (12, 53). Hence, the hypothetical pRb/E2F1-, pRb/E2F2-, or pRb/E2F3-regulated gene would function primarily in differentiation and not in the cell cycle. This proposed mechanism is consistent with the inability of R654W pRb to affect rod cell differentiation and the observation that a number of potential E2F1 target genes are involved in cellular differentiation (3). While other, unidentified pRb protein interactions lost in the R654W mutant may also be involved, our hypothesis makes the testable prediction that the compound loss *Rb1* and E2F1, E2F2, or E2F3 will rescue rod cell differentiation. Loss of E2F4 causes a cell-autonomous defect in erythrocyte maturation similar to that observed in *Rb1* null mice (20, 39). The fact that both *Rb1* and *E2F4* null mice exhibit an overlapping phenotype suggests that the pRb/E2F4 interaction may be required; the pRb/E2F4

complex may silence the expression of an inhibitor of erythrocyte maturation. This hypothesis is supported by the observations that R654W pRb retains the ability to stably bind E2F4 and that this correlates with improved erythrocyte maturation in R654W embryos. Additional reconstitution and conditional ablation experiments will be required to critically test this hypothesis since pRb also makes cell-extrinsic contributions to erythrocyte maturation. Id2 is an inhibitor of the tissue-restricted transcription factor PU.1, which controls the expression of genes important for macrophage differentiation (35). Binding of pRb to Id2 blocks Id2-mediated inhibition of PU.1, facilitating normal FLM differentiation in a cell-autonomous manner (21). Since R654W pRb retains the ability to interact with Id2, this mechanism is proposed to account for the improved FLM differentiation observed in R654W embryos.

The differential binding of R654W pRb to E2F4 and to E2F1, E2F2, and E2F3 reveals a previously unappreciated biochemical difference in the way pRb physically associates with different classes of E2F transcription factors. This observation also indicates that the R654W mutation does not cause a general loss of pRb protein binding activity but rather affects some protein interactions and leaves others unaffected. Since R654W pRb retains the ability to bind E2F4, the data also suggest that the pRb/E2F4 interaction is insufficient for pRb-mediated cell cycle control. The increased pRb/E2F4 association observed probably reflects decreased competition with E2F1, E2F2, and E2F3 for R654W pRb binding. Interpretation of phenotypes caused by mutation of *Rb1* therefore must account for the potential redistribution of pRb protein complexes and the possibility that this may elicit gain as well as loss of function. For example, in the absence of abundant interaction of pRb with E2F1, E2F2, and E2F3, R654W pRb may increase its interactions with other protein partners, potentially generating potentially novel functions. Likewise, *Rb1* mutant phenotypes must also be considered in the context of the pocket protein family. The two other pocket proteins, p107 and p130, share the ability to regulate the cell cycle through interaction with E2Fs. This functional overlap is reflected in the observation that the loss of all three pocket proteins causes cell cycle defects more pronounced than those caused by the loss of individual members (42). Functional compensation is also observed in vivo, as developmental defects associated with *Rb1* nullizygosity are exacerbated by the compound loss of p107 (26). While there is specificity in the preference of individual pocket proteins for binding different E2Fs, atypical pocket protein/E2F complexes can be observed in some situations (24). Thus, phenotypes observed upon *Rb1* mutation may be affected by redistribution of p107 and p130 complexes. Despite this, it is clear that pRb has unique functions, as only pRb is required for embryonic development. Further, only the loss of pRb is consistently associated with tumorigenesis in both mice and humans (7, 9). Among the molecular mechanisms utilized by the pocket proteins, those specific for pRb are likely to be particularly relevant to its unique role in embryonic development and tumor suppression.

ACKNOWLEDGMENTS

We thank Paul Soloway (Cornell University) and John Clifford (MD Anderson Cancer Center) for sharing plasmids. We acknowledge Karin Williams, Harold Love, Mary Vaughan, Jiakun Zhang, and Leyfou Dabo for technical advice. We acknowledge the Vanderbilt Mouse Metabolic Physiology Center for performing the fatty acid analysis.

This work was supported by grants from the NIH to D.W.G. (CA70292), S.W.H. (CA96403), and M.A.D. (EY014867). The Charlotte Geyer Foundation (D.W.G.), the American Lebanese Syrian Associated Charities (M.A.D.), and Research to Prevent Blindness (M.A.D.) also supported the work described. M.A.D. is a Pew Scholar.

REFERENCES

1. **Benevolenskaya, E. V., H. L. Murray, P. Branton, R. A. Young, and W. G. Kaelin.** 2005. Binding of pRB to the PHD protein RBP2 promotes cellular differentiation. Mol. Cell **18:**623–635.
2. **Blackshaw, S., S. Harpavat, J. Trimarchi, L. Cai, H. Huang, W. P. Kuo, G. Weber, K. Lee, R. E. Fraioli, S. H. Cho, R. Yung, E. Asch, L. Ohno-Machado, W. H. Wong, and C. L. Cepko.** 2004. Genomic analysis of mouse retinal development. PLoS Biol. **2:**1411–1431.
3. **Bracken, A. P., M. Ciro, A. Cocito, and K. Helin.** 2004. E2F target genes: unraveling the biology. Trends Biochem. Sci. **29:**409–417.
4. **Chan, H. M., L. Smith, and N. B. La Thangue.** 2001. Role of LXCXE motif-dependent interactions in the activity of the retinoblastoma protein. Oncogene **20:**6152–6163.
5. **Clark, A. J., K. M. Doyle, and P. O. Humbert.** 2004. Cell-intrinsic requirement for pRb in erythropoiesis. Blood **104:**1324–1326.
6. **Clarke, A. R., E. R. Maandag, M. van Roon, N. M. van der Lugt, M. van der Valk, M. L. Hooper, A. Berns, and H. te Riele.** 1992. Requirement for a functional Rb-1 gene in murine development. Nature **359:**328–330.
7. **Classon, M., and N. Dyson.** 2001. p107 and p130: versatile proteins with interesting pockets. Exp. Cell Res. **264:**135–147.
8. **Classon, M., and E. Harlow.** 2002. The retinoblastoma tumour suppressor in development and cancer. Nat. Rev. Cancer **2:**910–917.
9. **Cobrinik, D.** 2005. Pocket proteins and cell cycle control. Oncogene **24:**2796–2809.
10. **Dick, F. A., E. Sailhamer, and N. J. Dyson.** 2000. Mutagenesis of the pRB pocket reveals that cell cycle arrest functions are separable from binding to viral oncoproteins. Mol. Cell. Biol. **20:**3715–3727.
11. **Dimova, D. K., and N. J. Dyson.** 2005. The E2F transcriptional network: old acquaintances with new faces. Oncogene **24:**2810–2826.
12. **Donovan, S. L., and M. A. Dyer.** 2004. Developmental defects in Rb-deficient retinae. Vision Res. **44:**3323–3333.
13. **Dyer, M. A., and R. Bremner.** 2005. The search for the retinoblastoma cell of origin. Nat. Rev. Cancer **5:**91–101.
14. **Dyer, M. A., and C. L. Cepko.** 2001. p27Kip1 and p57Kip2 regulate proliferation in distinct retinal progenitor cell populations. J. Neurosci. **21:**4259–4271.
15. **Dyer, M. A., and C. L. Cepko.** 2001. The p57Kip2 cyclin kinase inhibitor is expressed by a restricted set of amacrine cells in the rodent retina. J. Comp. Neurol. **429:**601–614.
16. **Folch, J., M. Lees, and G. H. Sloane-Stanley.** 1957. A simple method for the isolation and purification of total lipides from animal tissues. J. Biol. Chem. **226:**497–509.
17. **Goodrich, D. W., N. P. Wang, Y. W. Qian, E. Y. Lee, and W. H. Lee.** 1991. The retinoblastoma gene product regulates progression through the G1 phase of the cell cycle. Cell **67:**293–302.
18. **Harbour, J. W.** 2001. Molecular basis of low-penetrance retinoblastoma. Arch. Ophthalmol. **119:**1699–1704.
19. **Harrington, E. A., J. L. Bruce, E. Harlow, and N. Dyson.** 1998. pRB plays an essential role in cell cycle arrest induced by DNA damage. Proc. Natl. Acad. Sci. USA **95:**11945–11950.
20. **Humbert, P. O., C. Rogers, S. Ganiatsas, R. L. Landsberg, J. M. Trimarchi, S. Dandapani, C. Brugnara, S. Erdman, M. Schrenzel, R. T. Bronson, and J. A. Lees.** 2000. E2F4 is essential for normal erythrocyte maturation and neonatal viability. Mol. Cell **6:**281–291.
21. **Iavarone, A., E. R. King, X. M. Dai, G. Leone, E. R. Stanley, and A. Lasorella.** 2004. Retinoblastoma promotes definitive erythropoiesis by repressing Id2 in fetal liver macrophages. Nature **432:**1040–1045.
22. **Jacks, T., A. Fazeli, E. M. Schmitt, R. T. Bronson, M. A. Goodell, and R. A. Weinberg.** 1992. Effects of an Rb mutation in the mouse. Nature **359:**295–300.
23. **Ji, P., H. Jiang, K. Rekhtman, J. Bloom, M. Ichetovkin, M. Pagano, and L. Zhu.** 2004. An Rb-Skp2-p27 pathway mediates acute cell cycle inhibition by Rb and is retained in a partial-penetrance Rb mutant. Mol. Cell **16:**47–58.
24. **Lee, E. Y., H. Cam, U. Ziebold, J. B. Rayman, J. A. Lees, and B. D. Dynlacht.** 2002. E2F4 loss suppresses tumorigenesis in Rb mutant mice. Cancer Cell **2:**463–472.
25. **Lee, E. Y., C. Y. Chang, N. Hu, Y. C. Wang, C. C. Lai, K. Herrup, and W. H. Lee.** 1992. Mice deficient for Rb are nonviable and show defects in neurogenesis and haematopoiesis. Nature **359:**288–294.
26. **Lee, M. H., B. O. Williams, G. Mulligan, S. Mukai, R. T. Bronson, N. Dyson,**

E. Harlow, and T. Jacks. 1996. Targeted disruption of p107: functional overlap between p107 and Rb. Genes Dev. **10:**1621–1632.
27. **Li, Y., X. Wang, X. Zhang, and D. W. Goodrich.** 2005. Human hHpr1/p84/Thoc1 regulates transcriptional elongation and physically links RNA polymerase II and RNA processing factors. Mol. Cell. Biol. **25:**4023–4033.
28. **Lohmann, D. R., B. Brandt, W. Hopping, E. Passarge, and B. Horsthemke.** 1994. Distinct RB1 gene mutations with low penetrance in hereditary retinoblastoma. Hum. Genet. **94:**349–354.
29. **Maandag, E. C., M. van der Valk, M. Vlaar, C. Feltkamp, J. O'Brien, M. van Roon, L. N. van der Lugt, A. Berns, and H. te Reile.** 1994. Developmental rescue of an embryonic-lethal mutation in the retinoblastoma gene in chimeric mice. EMBO J. **13:**4260–4268.
30. **MacPherson, D., J. Sage, T. Kim, D. Ho, M. E. McLaughlin, and T. Jacks.** 2004. Cell type-specific effects of Rb deletion in the murine retina. Genes Dev. **18:**1681–1694.
31. **Marino, S., M. Vooijs, H. van Der Gulden, J. Jonkers, and A. Berns.** 2000. Induction of medulloblastomas in p53-null mutant mice by somatic inactivation of Rb in the external granular layer cells of the cerebellum. Genes Dev. **14:**994–1004.
32. **Miccadei, S., C. Provenzano, M. Mojzisek, P. G. Natali, and D. Civitareale.** 2005. Retinoblastoma protein acts as Pax 8 transcriptional coactivator. Oncogene **24:**6993–7001.
33. **Morrison, W. R., and L. M. Smith.** 1964. Preparation of fatty acid methyl esters and dimethylacetals from lipids with boron fluoride-methanol. J. Lipid Res. **5:**600–608.
34. **Neuman, E., E. K. Flemington, W. R. Sellers, and W. G. Kaelin, Jr.** 1994. Transcription of the E2F-1 gene is rendered cell cycle dependent by E2F DNA-binding sites within its promoter. Mol. Cell. Biol. **14:**6607–6615.
35. **Oikawa, T., T. Yamada, F. Kihara-Negishi, H. Yamamoto, N. Kondoh, Y. Hitomi, and Y. Hashimoto.** 1999. The role of Ets family transcription factor PU.1 in hematopoietic cell differentiation, proliferation and apoptosis. Cell Death Differ. **6:**599–608.
36. **Onadim, Z., A. Hogg, P. N. Baird, and J. K. Cowell.** 1992. Oncogenic point mutations in exon 20 of the RB1 gene in families showing incomplete penetrance and mild expression of the retinoblastoma phenotype. Proc. Natl. Acad. Sci. USA **89:**6177–6181.
37. **Otterson, G. A., W. Chen, A. B. Coxon, S. N. Khleif, and F. J. Kaye.** 1997. Incomplete penetrance of familial retinoblastoma linked to germ-line mutations that result in partial loss of RB function. Proc. Natl. Acad. Sci. USA **94:**12036–12040.
38. **Otterson, G. A., S. Modi, K. Nguyen, A. B. Coxon, and F. J. Kaye.** 1999. Temperature-sensitive RB mutations linked to incomplete penetrance of familial retinoblastoma in 12 families. Am. J. Hum. Genet. **65:**1040–1046.
39. **Rempel, R. E., M. T. Saenz-Robles, R. Storms, S. Morham, S. Ishida, A. Engel, L. Jakoi, M. F. Melhem, J. M. Pipas, C. Smith, and J. R. Nevins.** 2000. Loss of E2F4 activity leads to abnormal development of multiple cellular lineages. Mol. Cell **6:**293–306.
40. **Saavedra, H. I., L. Wu, A. de Bruin, C. Timmers, T. J. Rosol, M. Weinstein, M. L. Robinson, and G. Leone.** 2002. Specificity of E2F1, E2F2, and E2F3 in mediating phenotypes induced by loss of Rb. Cell Growth Differ. **13:**215–225.
41. **Sage, J., A. L. Miller, P. A. Perez-Mancera, J. M. Wysocki, and T. Jacks.** 2003. Acute mutation of retinoblastoma gene function is sufficient for cell cycle re-entry. Nature **424:**223–228.
42. **Sage, J., G. J. Mulligan, L. D. Attardi, A. Miller, S. Chen, B. Williams, E. Theodorou, and T. Jacks.** 2000. Targeted disruption of the three Rb-related genes leads to loss of G(1) control and immortalization. Genes Dev. **14:**3037–3050.
43. **Schweers, B. A., and M. A. Dyer.** 2005. Perspective: new genetic tools for studying retinal development and disease. Vis. Neurosci. **22:**553–560.
44. **Sellers, W. R., B. G. Novitch, S. Miyake, A. Heith, G. A. Otterson, F. J. Kaye, A. B. Lassar, and W. G. Kaelin, Jr.** 1998. Stable binding to E2F is not required for the retinoblastoma protein to activate transcription, promote differentiation, and suppress tumor cell growth. Genes Dev. **12:**95–106.
45. **Spike, B. T., A. Dirlam, B. C. Dibling, J. Marvin, B. O. Williams, T. Jacks, and K. F. Macleod.** 2004. The Rb tumor suppressor is required for stress erythropoiesis. EMBO J. **23:**4319–4329.
46. **Takahashi, C., R. T. Bronson, M. Socolovsky, B. Contreras, K. Y. Lee, T. Jacks, M. Noda, R. Kucherlapati, and M. E. Ewen.** 2003. *Rb* and N-*ras* function together to control differentiation in the mouse. Mol. Cell. Biol. **23:**5256–5268.
47. **Thomas, D. M., S. A. Carty, D. M. Piscopo, J. S. Lee, W. F. Wang, W. C. Forrester, and P. W. Hinds.** 2001. The retinoblastoma protein acts as a transcriptional coactivator required for osteogenic differentiation. Mol. Cell **8:**303–316.
48. **Tsai, K. Y., Y. Hu, K. F. Macleod, D. Crowley, L. Yamasaki, and T. Jacks.** 1998. Mutation of E2f-1 suppresses apoptosis and inappropriate S phase entry and extends survival of Rb-deficient mouse embryos. Mol. Cell **2:**293–304.
49. **Whitaker, L. L., H. Su, R. Baskaran, E. S. Knudsen, and J. Y. J. Wang.** 1998. Growth suppression by an E2F-binding-defective retinoblastoma protein (RB): contribution from the RB C pocket. Mol. Cell. Biol. **18:**4032–4042.
50. **Williams, B. O., E. M. Schmitt, L. Remington, R. T. Bronson, D. M. Albert, R. A. Weinberg, and T. Jacks.** 1994. Extensive contribution of Rb-deficient cells to adult chimeric mice with limited histopathological consequences. EMBO J. **13:**4251–4259.
51. **Wu, L., A. de Bruin, H. I. Saavedra, M. Starovic, A. Trimboli, Y. Yang, J. Opavska, P. Wilson, J. C. Thompson, M. C. Ostrowski, T. J. Rosol, L. A. Woollett, M. Weinstein, J. C. Cross, M. L. Robinson, and G. Leone.** 2003. Extra-embryonic function of Rb is essential for embryonic development and viability. Nature **421:**942–947.
52. **Wu, L., C. Timmers, B. Maiti, H. I. Saavedra, L. Sang, G. T. Chong, F. Nuckolls, P. Giangrande, F. A. Wright, S. J. Field, M. E. Greenberg, S. Orkin, J. R. Nevins, M. L. Robinson, and G. Leone.** 2001. The E2F1-3 transcription factors are essential for cellular proliferation. Nature **414:**457–462.
53. **Zhang, J., J. Gray, L. Wu, G. Leone, S. Rowan, C. L. Cepko, X. Zhu, C. M. Craft, and M. A. Dyer.** 2004. Rb regulates proliferation and rod photoreceptor development in the mouse retina. Nat. Genet. **36:**351–360.
54. **Ziebold, U., T. Reza, A. Caron, and J. A. Lees.** 2001. E2F3 contributes both to the inappropriate proliferation and to the apoptosis arising in Rb mutant embryos. Genes Dev. **15:**386–391.